



ELSEVIER

Journal of Nuclear Materials 275 (1999) 318–323

Journal of  
nuclear  
materials

www.elsevier.nl/locate/jnucmat

# Diffusion-controlled hydride growth near crack tip in zirconium under temperature transients

S.-Q. Shi\*

*Department of Mechanical Engineering, The Hong Kong Polytechnic University, Kowloon, Hong Kong, People's Republic of China*

Received 9 February 1999; accepted 15 May 1999

## Abstract

Hydride precipitation at stress concentrators such as crack tips in the zirconium alloys is a concern in nuclear power industry, since this diffusion-controlled process may lead to slow crack growth, even failure of structural components. A nonlinear diffusion model has been developed to simulate the moving boundary problem of a growing hydride at crack tip. Results show that this model provides reasonable predictions on the hydride growth behavior under temperature transients. © 1999 Elsevier Science B.V. All rights reserved.

## 1. Introduction

In hydride-forming metals used for structural and pressure containing components, one concern is the formation and fracture of metal hydrides at flaws [1,2]. The physical processes involved in this phenomenon are as follows. Hydrogen atoms diffuse to the tensile region at the flaw. If the hydrogen concentration in this region reaches its solubility limit, hydrides will start to form and grow. When this hydrided zone reaches a critical size under a sufficient tensile stress, fracture through this zone can occur. This process, called delayed hydride cracking (or DHC), can then repeat itself, and could eventually result in mechanical failure of the structural component.

It is clear that, in order to understand DHC, three distinct physical phenomena need to be understood: (1) hydrogen diffusion in a stress field; this controls the rate of DHC; (2) hydride phase transformation involving a large misfit strain between hydride and matrix; this determines the hysteresis in the solvus boundaries and the history effect of DHC; and (3) micromechanics of hydride cracking; this determines the criteria for the initiation of DHC. Over the years, there have been extensive experimental and theoretical studies of DHC. Progress in understanding DHC has been made in all three areas

discussed above [3]. This paper is focussed on the phenomenon relevant to DHC: the diffusion-controlled hydride growth at a sharp crack tip under temperature transients. To study and simulate this process, knowledge of these three phenomena is necessary.

The time-dependent hydride growth at a crack tip at a constant temperature has been simulated by Metzger [4] and Lufrano et al. [5] using finite element methods, and by Shi et al. [6] using a partial-differential-equation (PDE) solver. Quite often, the structural components experience stress and/or temperature cycles as a consequence of normal operation. Since the hydrogen diffusivity and solubility change with temperature, large temperature variations will have major effects on hydrogen diffusion and hydride formation, which in turn will have impacts on DHC. In the next section, the computer modeling using a PDE solver for the time-dependent growth of a hydride at a sharp crack is briefly summarized. Then the temperature dependence of hydrogen solubility in zirconium is discussed, because this issue is crucial in the formulation of physical constraints for solving the problem. Finally, some simulation examples and discussion of the time-dependent growth of hydrides under temperature transients are given.

## 2. Mathematical model

Fick's first and second laws are applied to study the diffusion of hydrogen to a crack tip under tensile stress.

\* Tel.: +852 2766 7821; fax: +852 2365 4703.

E-mail address: mmsqshi@polyu.edu.hk (S.-Q. Shi).

Following the work by Dutton and Puls [7], the stress field is assumed to be cylindrically symmetric, loaded in tension under plane strain condition, as schematically shown in Fig. 1. In zirconium alloys, the hydride formed at a crack tip can be idealized as having a plate-like shape of a rectangular prism. Since the backward growth of the hydride to the left in Fig. 1 is limited by the crack tip, we use the half length ( $r_h$ ) of the hydride disk to approximate the total length of the hydride growing away from the crack. For a hydride with thickness  $\delta$  and length  $r_h$ , its growth rate equals to the rate of hydrogen atoms arriving at  $r_h$  (the interface between matrix and the hydride) multiplied by the hydride volume per hydrogen atom,  $\Omega_{\text{hyd}}$ . This results in [6]

$$dr_h/dt = -(\pi \cdot r_h/\delta)\Omega_{\text{hyd}}\rho_{\text{Zr}}J(r = r_h, t), \quad (1)$$

where  $t$  is time,  $\rho_{\text{Zr}}$  the number of Zr atoms per unit volume, and  $J(r, t)$  is the flux of hydrogen in the unit of at.% H  $\text{m}^{-2} \text{s}^{-1}$ .  $J(r, t)$  is determined by Fick's first law

$$J(r, t) = -D_H \nabla u(r, t) + [D_H u(r, t)/RT]F(r), \quad (2)$$

where  $D_H$  is the hydrogen diffusivity,  $T$  the absolute temperature,  $R$  the gas constant,  $u(r, t)$  the hydrogen concentration in at.%, and  $F(r)$  is the driving force due to the hydrostatic stress field around the crack. For zirconium,  $F(r)$  can be approximated by

$$F(r) \approx -\bar{V}_H \nabla \left[ \frac{1}{3} \sum_{i=1}^3 \sigma_{ii} \right] = -\frac{A}{2} r^{-3/2} \quad (r \geq r_p) \quad (3)$$

$$\approx \text{constant} = -\frac{A}{2} r_p^{-3/2} \quad (r < r_p)$$

and

$$A = 2\bar{V}_H(1 + \nu)K_I/3\sqrt{2\pi}. \quad (4)$$

Here,  $\bar{V}_H$  is the molar volume of hydrogen in solid solution,  $\nu$  the Poisson's ratio,  $K_I$  the mode-I stress intensity factor and  $\sigma_{ii}$  the principal stresses. The distance,  $r_p$ ,

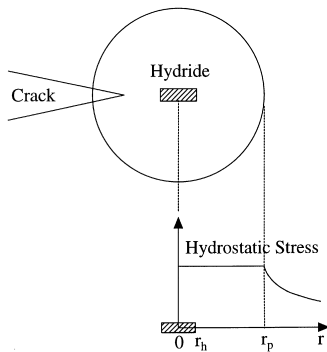


Fig. 1. The assumed hydrostatic stress profile at crack tip in zirconium.

is the plastic zone size along the crack plane under plane strain, which is given by [8]

$$r_p = [(1 - 2\nu)^2/2\pi](K_I/\sigma_{\text{ys}})^2, \quad (5)$$

where  $\sigma_{\text{ys}}$  is the yield strength of the matrix.

In Eq. (2),  $u(r, t)$  can be evaluated by Fick's second law, i.e., in a cylindrical system,

$$\partial u(r, t)/\partial t = -(1/r)\nabla[r \cdot J(r, t)], \quad (6)$$

$$r_h(t) \leq r \leq L + r_h(t),$$

where  $r_h$  is defined as the position of the hydride tip and is a function of time and  $L$  is the effective length of the diffusion field which depends on the geometry of the specimen or the time allowed for diffusion.

With proper initial condition (IC) and boundary conditions (BC), Eqs. (1)–(6) define a moving-boundary diffusion problem that evaluates the hydrogen distribution around crack,  $u(r, t)$ ; hydrogen influx to the crack tip,  $J(r, t)$ ; and the hydride length,  $r_h(t)$ , as functions of stress intensity factor, material properties (yield stress, Poisson's ratio and diffusivity, etc.), hydrogen concentration (through IC and BC) and temperature (through material properties). For numerical simulations, this moving boundary problem can be converted into a fixed boundary condition by introducing a new variable,  $x$ , as following.

When  $r_h < r_p$ , let

$$x = \frac{r - r_h}{r_p - r_h} \alpha \quad \text{if } r_h < r < r_p (0 < x < \alpha)$$

$$= \frac{r - r_p}{L - r_p + r_h} \beta + \alpha \quad \text{if } r_p \leq r < L + r_h (\alpha \leq x < \beta + \alpha), \quad (7)$$

where  $\alpha$  and  $\beta$  are arbitrary constants. Then Eq. (6) takes the form

$$\{\partial u(x, t)/\partial t - [\partial u(x, t)/\partial x][(\alpha - x)/(r_p - r_h(t))]dr_h/dt\}$$

$$\times \{(x/\alpha)[r_p - r_h(t) + r_h]\{r_p - r_h(t)\}/\alpha$$

$$= -(\partial/\partial x)\{[(x/\alpha)[r_p - r_h(t) + r_h]J(x, t)\} \quad (8a)$$

for  $0 < x < \alpha$ , and,

$$\{\partial u(x, t)/\partial t - [\partial u(x, t)/\partial x][(x - \alpha)/(L - r_p + r_h(t))]dr_h/dt\}$$

$$\times \{[(x - \alpha)/\beta][L - r_p + r_h(t) + r_p]\{L - r_p + r_h(t)\}/\beta$$

$$= -(\partial/\partial x)\{[(x - \alpha)/\beta][L - r_p + r_h(t) + r_p]J(x, t)\} \quad (8b)$$

for  $\alpha \leq x < \alpha + \beta$ . And (2) becomes

$$J(x, t) = -D_H[\partial u(x, t)/\partial x]\alpha/[r_p - r_h(t)], \quad \text{for } 0 < x < \alpha$$

$$= -D_H\{[\partial u(x, t)/\partial x]\beta/[L - r_p + r_h(t) + (A/2RT)$$

$$\times u(x, t)[[(x - \alpha)/\beta][L - r_p + r_h(t) + r_p]^{-3/2}\}, \quad (9)$$

for  $\alpha \leq x < \alpha + \beta$ .

When  $r_h \geq r_p$ , let

$$x = r - r_h. \quad (10)$$

Then PDE Eq. (6) becomes,

$$\begin{aligned} \{ \partial u(x, t) / \partial t - [\partial u(x, t) / \partial x] dr_h / dt \} (x + r_h) \\ = -(\partial / \partial x) [(x + r_h) J(x, t)], \end{aligned} \quad (11)$$

where

$$\begin{aligned} J(x, t) = -D_H \{ \partial u(x, t) / \partial x + (A / 2RT) u(x, t) \\ \times (x + r_h)^{-3/2} \}. \end{aligned} \quad (12)$$

Fig. 2 presents a simulation result for the hydride growth rate as a function of stress intensity factor,  $K_I$ . The effective length of the diffusion field was chosen to be 2 mm. The model reflects experimental observations by Dutton et al. [9] that DHC is stopped when  $K_I$  is below a threshold value,  $K_{IH}$ .

### 3. Hysteresis of hydrogen solubility in Zr

The IC and BC of the above problem are usually defined by the amount of hydrogen in solid solution. The amount of hydrogen in solid solution, on the other hand, depends on the total hydrogen concentration in the component, temperature as well as its immediate thermal history. This is because there is a strong hysteresis in hydrogen solubility in zirconium. At a given temperature, the hydrogen solubility for hydride formation,  $C^f$ , measured on cooling down the component is significantly higher than the hydrogen solubility for hydride dissolution,  $C^d$ , measured on heating up the component. Both  $C^f$  and  $C^d$  are found to follow the following relationship in the temperature range of 100–300°C,

$$C^f = A \exp[-\bar{Q}^f / RT] \quad (13)$$

and

$$C^d = B \exp[-\bar{Q}^d / RT], \quad (14)$$

where  $A$  and  $B$  are pre-exponential constants, and  $\bar{Q}^f$  and  $\bar{Q}^d$  are molar free energies for hydride formation and dissolution, respectively, which are derived from experiments, see Fig. 3. According to the widely cited work by Kearns [10] and Slattery [11], the absolute value of  $\bar{Q}^d$  is larger than that of  $\bar{Q}^f$ . The relationships Eqs. (13) and (14) may be dependent on the cooling rate. However, for a cooling or heating rate of less than 2°C per minutes used in this study, these relationships are not sensitive to the rate of temperature transients [12].

These two lines represent the phase boundaries. The  $C^d$  line represents the solubility limit when hydrides are dissolving during heating, while the  $C^f$  line represents the solubility limit when hydrides are precipitating during cooling. Because of the existence of these two lines, the concentration of hydrogen in solution depends on the thermal history. On cooling from high temperatures where all hydrogen atoms are in solution, hydrides will not start to form until the temperature reaches the  $C^f$  line. Therefore, the amount of hydrogen in solution for this process can be represented by a horizontal line in Fig. 3, from point 1 to point 2. On further cooling, the amount of hydrogen in solution would follow the  $C^f$  line (from 2 to 3). If one starts to heat the component from point 3, the amount of hydrogen in solution will not increase until the temperature reaches the  $C^d$  line (from 3 to 4). Further heating would increase the amount of hydrogen in solution along the  $C^d$  line until it reaches the temperature where all hydrides are dissolved (back to the level of point 1).

The reasons for this hysteresis are beyond the scope of this paper. Simply speaking, it is related to plastic

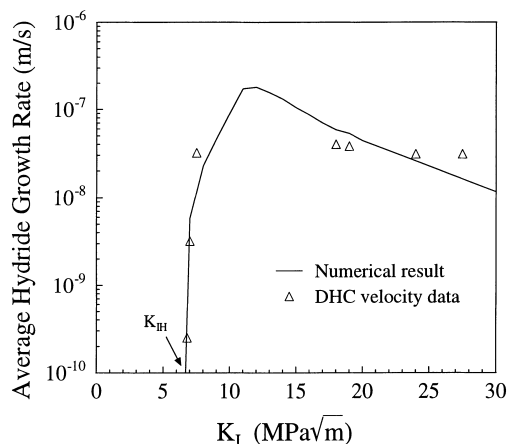


Fig. 2. Average hydride growth rate as a function of  $K_I$ .  $T = 523$  K and  $\sigma_{ys} = 375$  MPa, compared with experimental DHC velocity data by Dutton et al. [9].

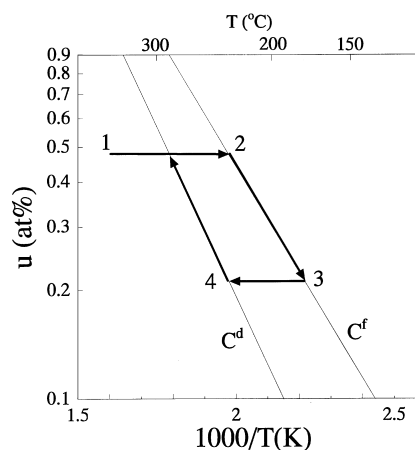


Fig. 3. Hysteresis in hydrogen solubility in Zr.

deformation during hydride formation and dissolution. For more detail, readers are referred to Birnbaum et al. [13], Flanagan and Clewley [14], Puls [15], and Leitch and Shi [16]. It should be noted that the high tensile hydrostatic stress at the crack tip attracts hydrogen atoms so that the hydrogen concentration in solution at the crack tip will be higher than the average hydrogen concentration in solution in the bulk. Therefore it is possible for hydrides to form at higher temperatures at crack tips than in the bulk. The details of this shift for hydride formation at a crack tip depend on material properties such as the yield strength, loading level and history, the geometry of the crack, and the rate of stress and/or temperature transients.

The hydride phase transformation involves the stages for nucleation and growth. For the purpose of engineering assessment for nuclear power plants, we choose to use the experimental relationships Eqs. (13) and (14) to determine the onset of hydride formation or dissolution during a temperature transient, while making no distinction between the stages of nucleation and growth. In the following, we demonstrate, based on the solubility limits given above, the method and technique used to determine hydride formation and growth at a crack.

#### 4. Examples of hydride growth under temperature transients

##### 4.1. Hydride growth during cooling

Take a Zr–2.5Nb pressure tube material used in CANDU pressurized heavy water reactor as an example. Assume that the material has picked up 0.48 at.% of deuterium in solution during service in reactor and starts to cool from 300°C to 200°C under a cooling rate of 105°C/h. Also assume that the pressure tube has a crack-like flaw along the axial direction with a stress intensity factor  $K_I = 15 \text{ MPa m}^{1/2}$ . We want to know the amount of hydrides (in this case, deuterides) accumulated at the crack tip in this cooling process. Material constants are given in Table 1. The external load (i.e., internal pressure in the tube) is applied at normal operating condition at the beginning of the cooling process. This implies that the plastic zone size is approximately fixed at 300°C, because the yield strength is smaller at higher temperatures. The diffusivity data are taken from Kearns [17] for hydrogen, modified to take the isotope effect into account. We also assume that the average thickness of the crack-tip hydride is 3  $\mu\text{m}$  and the effective length of the diffusion field  $L$  is 3 mm. Therefore, IC is

$$u(r, t = 0) = 0.48 \text{ at.}\% \quad 0 \leq r_h \leq L. \quad (15)$$

Table 1  
Constants used in simulations

$R = 8.3144 \text{ J mol}^{-1} \text{ K}^{-1}$
$v = 0.436 - 4.8 \times 10^{-4}(T - 300)$
$\sigma_{ys} = 988 - 1.154 \cdot T \text{ MPa}$
$\Omega_{\text{hyd}} = 1.643 \times 10^{-29} \text{ m}^3/\text{H}$
$\rho_{\text{Zr}} = 4.285 \times 10^{28} \text{ atoms m}^3$
$D_{\text{H}} = 5.468 \times 10^{-7} \exp(-45293/\text{RT}) \text{ m}^2 \text{ s}^{-1}$
$C^f = 208.5 \exp(-3071/T) \text{ at.}\%$
$C^d = 1080 \exp(-4318/T) \text{ at.}\%$
$\bar{V}_{\text{H}} = 16.7 \times 10^{-7} \text{ m}^3 \text{ mol}^{-1}$

And the BCs are

$$\text{Left : } J(r = 0, t) = 0 \quad \text{if } r_h = 0 \quad (16a)$$

(No hydride is formed)

or,

$$u(r = r_h, t) = C^f \quad \text{if } r_h > 0 \quad (16b)$$

(A hydride has formed)

$$\text{Right : } J(r = L + r_h, t) = 0. \quad (17)$$

Two more physical constraints are (i) deuterium in solution cannot exceed  $C^f$  at any point in the diffusion field and at any temperature (otherwise hydrides would form), and (ii) deuterium in solution cannot be lower than  $C^d$  at any point unless it is at the temperatures where all the hydrides are dissolved (when  $u(r, t) = 0.48 \text{ at.}\%$ ), i.e.,

$$u(r, t) \leq C^f \quad (18)$$

$$u(r, t) \geq C^d \quad \text{if } u(r, t) < 0.48 \text{ at.}\% \quad (19)$$

To actually fulfill these two conditions, one has to set small time intervals or small temperature steps (about 1°C in this example) during the simulation. The simulation result is shown in Fig. 4 in terms of the hydrided area in plane strain.

As can be seen, at high temperatures, no hydride is formed and all deuterium atoms are in solid solution. The crack-tip hydride starts to form at about 257°C at which temperature no hydride should form in the bulk. According to  $C^f$  data, bulk hydrides should form at about 235°C, see Fig. 5. Hydride formation at the crack tip is possible because the deuterium concentration in solution at the crack tip is much higher (about 0.64 at.%) than in the bulk (0.48 at.%). Suppose that we stop the cooling and start to heat the material from 257°C. Then this small crack-tip hydride would not dissolve until the temperature reaches about 308°C, because  $C^d = 0.64 \text{ at.}\%$  at this temperature, Fig. 5. Therefore the presence of a crack increases the local temperature for hydride dissolution from 292°C for bulk hydrides by about 16°C.

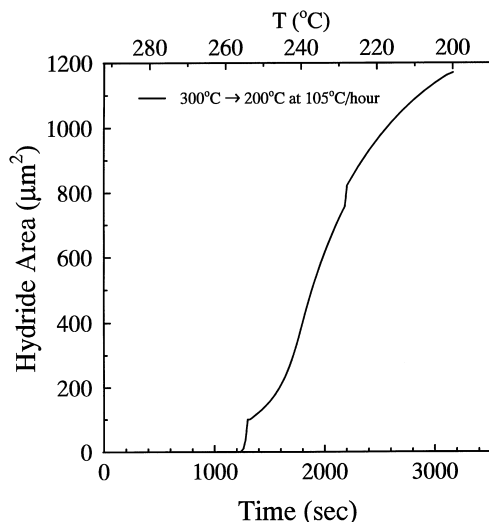


Fig. 4. Hydride growth at a crack tip during cooling.

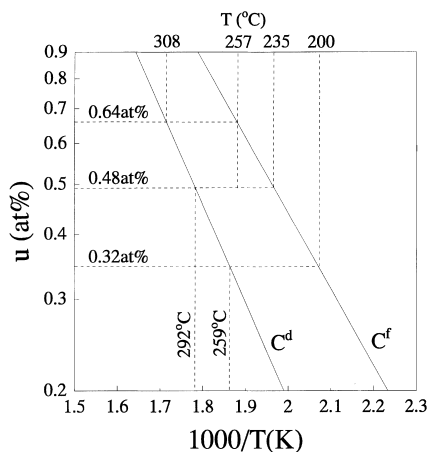


Fig. 5. Effects of crack tip stress field on hydride solubility for dissolving and precipitating hydrides.

Also based on Fig. 4, the initial growth rate for the crack-tip hydride is fast when the hydride length ( $r_h$ ) is crossing the plastic zone boundary ( $r_p$ ) where the driving force from the hydrostatic stress gradient is a maximum. The rate slows down at lower temperatures due to a combination of lower diffusion rate and longer hydride length (at such a distance the stress gradient is relatively small). This type of behavior is consistent with observations from DHC experiments.

It should be noted that the starting temperature for hydride formation is controlled by the total hydrogen in solution, cooling rate and material properties. Therefore this method can be used to evaluate the effects of each factor on the onset of hydride formation during cooling.

If the cooling rate is low enough as compared to the diffusion rate, another relatively simple analytical method for estimating hydride formation temperature can also be used [18].

In this example, we did not allow the crack-tip hydride to fracture during cooling. Therefore, the stress distribution as well as plastic zone size is approximately fixed at the level that existed at high temperature (300°C). Experimental evidence and current theory for DHC suggest that, once the hydride reaches a critical length, fracture through the hydride should occur, and hydrogen diffusion and hydride growth will begin again from the fresh crack tip. In this case, the newly created crack tip would have a smaller plastic zone size (higher yield strength at lower temperatures) and a greater stress gradient. These types of simulations can be done using the above numerical method, but one needs to add one more physical constraint: i.e., the simulation stops when the hydride reaches its critical length. The ratio of critical hydride length ( $r_h$ ) to the time spent provides the estimation of DHC velocity. At this point, the stress distribution shall be updated and the simulation restarted from the new crack tip. Fig. 6 presents an example of such simulation (a critical hydride length of 20  $\mu\text{m}$  is assumed) and compares with experimental results on DHC velocity measured by Eadie et al. [19]. In this simulation, a constant critical hydride length and a constant hydride thickness at all temperatures were assumed. However, it is believed that the critical hydride length and hydride thickness vary with temperature. For a better simulation, the knowledge of dependence of hydride shape on temperature is required.

Another practical problem in operating a power station is to determine the holding time at an intermediate temperature as compared to at cold temperature for maintenance purposes. Among other factors to be

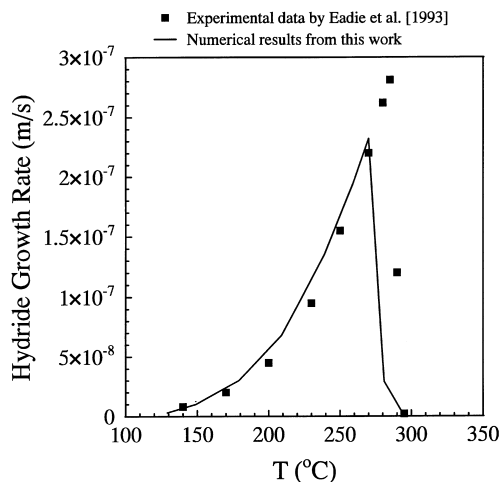


Fig. 6. Hydride growth rate at crack tip during cooling.

considered, a postulated flaw is usually assessed using the aforementioned method. In such assessment, combinations of cooling and holding are simulated for different holding temperatures. And an acceptable holding time can be found based on conservative assumptions about amount of hydride accumulated at the flaw.

#### 4.2. Hydride growth during heating

Hydride growth during heating is less worrisome in practice because most experiments have shown that DHC will stop at an early stage of heating process. Nevertheless, the current model can simulate the heating process quite satisfactorily.

Suppose that the same component in Fig. 5 is heated from 200°C back to 300°C at the same rate. Again, we want to know the additional amount of hydrides accumulated at the crack tip. In this case, the BCs are the same as during cooling (Eqs. (16a)–(17)) but the initial condition is very important for the possible outcomes of the simulation.

If the final deuterium distribution and hydride length from cooling are taken as the IC, one would find that the hydride will not grow any further at all during heating, because the hydride growth has already saturated at 200°C upon cooling. However, this hydride will not dissolve until temperature reaches about 259°C, because this is the dissolving temperature for a deuterium concentration of 0.32 at.% in solution which is fixed by the  $C^f$  line at 200°C (see Fig. 5).

On the other hand, if one assumes that the hydride had fractured at 200°C and the simulation is started at a fresh crack tip (stress update is required), then according to the simulation the crack-tip hydride will form and grow up to 209°C to a length of 20  $\mu\text{m}$ . If the hydride fractures again (i.e., the hydride reaches the critical length for DHC at this temperature), then a new hydride will form and start to grow again up to a new temperature of 217°C. Such a process can repeat itself until the temperature is high enough so that the crack-tip hydride cannot grow to its critical length. With knowledge of the critical hydride length, one can use this method to estimate the arrest temperature for DHC during heating. This arrest temperature should be lower than the DHC starting temperature during cooling (257°C), because the hydrogen concentration in solution during heating from 200°C (0.32 at.%) is much lower than during cooling from 300°C (0.48 at.%). These results qualitatively agree with experimental observations.

## 5. Conclusions

A numerical diffusion model is developed to simulate hydride growth at a crack tip under temperature transients. It is demonstrated that this method can be used to estimate the amount of hydrides accumulated at the crack tip during cooling and heating. With knowledge of the critical hydride length for DHC, this method can also be used to estimate the crack growth during temperature transients and the initiation or arrest temperatures for DHC. These estimates are important for the assessment of the lifetime of a structural component that is made of hydride-forming metals or alloys.

## References

- [1] R. Dutton, Hydrogen in Metals, The Metallurgical Society of CIM Annual Volume, 1978, p. 16.
- [2] H.K. Birnbaum, in: N.R. Moody, A.W. Thompson (Eds.), Hydrogen Effects on Material Behavior, TMS, 1989, p. 639.
- [3] S.-Q. Shi, M.P. Puls, Advances in the theory of delayed hydride cracking, in: N.R. Moody, A.W. Thompson (Eds.), Hydrogen Effects on Material Behavior, TMS, 1996, pp. 611–621.
- [4] D.R. Metzger, Ontario Hydro Technologies Report, No. 91-102K, 1991.
- [5] J. Lufano, P. Sofronis, H.K. Birnbaum, J. Mech. Phys. Solids 44 (2) (1996) 179.
- [6] S.-Q. Shi, M. Liao, M.P. Puls, Modelling Simul. Mater. Sci. Eng. 2 (1994) 1065.
- [7] R. Dutton, M.P. Puls, in: A.W. Thompson, I.M. Bernstein (Eds.), Effect of Hydrogen on Behavior of Materials, 1976, p. 512.
- [8] T.M. Banks, A. Garlick, Eng. Fracture Mech. 19 (1984) 571.
- [9] R. Dutton, K. Nuttall, M.P. Puls, L.A. Simpson, Metall. Trans. A8 (1977) 1553.
- [10] J.J. Kearns, J. Nucl. Mater. 22 (1967) 292.
- [11] G.F. Slatery, J. Inst. Met. 95 (1967) 43.
- [12] Z.L. Pan, I.G. Ritchie, M.P. Puls, AecL Whiteshell Lab., Pinawa, Manitoba, Canada, unpublished research, 1993.
- [13] H.K. Birnbaum, M.L. Grossbeck, M. Amano, J. Less-Common Met. 49 (1976) 357.
- [14] T.B. Flanagan, J.D. Clewley, J. Less-Common Met. 83 (1982) 127.
- [15] M.P. Puls, Metall. Trans. A21 (1989) 2905.
- [16] B.W. Leitch, S.Q. Shi, Modelling Simul. Mater. Sci. Eng. 4 (1996) 281.
- [17] J.J. Kearns, J. Nucl. Mater. 43 (1972) 330.
- [18] S.-Q. Shi, G.K. Shek, M.P. Puls, J. Nucl. Mater. 218 (1995) 189.
- [19] R.L. Eadie, D.R. Metzger, M. Leger, Scr. Metall. 29 (1993) 335.